

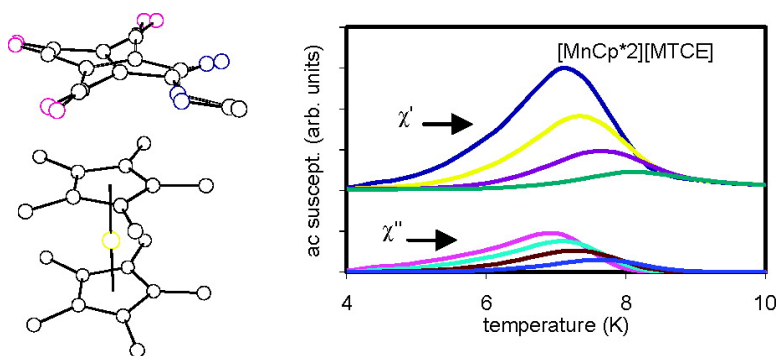
Article

A Family of Decamethylmetallocene Charge-Transfer Salt Magnets Using Methyl Tricyanoethylenecarboxylate (MTCE) as the Electron Acceptor

Guangbin Wang, Carla Slebodnick, Ray J. Butcher, Mary C. Tam, T. Daniel Crawford, and Gordon T. Yee

J. Am. Chem. Soc., **2004**, 126 (51), 16890-16895 • DOI: 10.1021/ja0457213 • Publication Date (Web): 03 December 2004

Downloaded from <http://pubs.acs.org> on April 5, 2009



More About This Article

Additional resources and features associated with this article are available within the HTML version:

- Supporting Information
- Links to the 4 articles that cite this article, as of the time of this article download
- Access to high resolution figures
- Links to articles and content related to this article
- Copyright permission to reproduce figures and/or text from this article

[View the Full Text HTML](#)

A Family of Decamethylmetallocene Charge-Transfer Salt Magnets Using Methyl Tricyanoethylenecarboxylate (MTCE) as the Electron Acceptor

Guangbin Wang,[†] Carla Slebodnick,[†] Ray J. Butcher,[‡] Mary C. Tam,[†]
T. Daniel Crawford,[†] and Gordon T. Yee^{*,†}

Contribution from the Virginia Polytechnic Institute and State University,
Blacksburg, Virginia 24061, and Howard University, Washington, D.C. 20059

Received July 16, 2004; E-mail: gyee@vt.edu

Abstract: Methyl tricyanoethylenecarboxylate, MTCE, has been used as a one-electron acceptor building block for the synthesis of isomorphous decamethylmetallocene charge-transfer salt magnets of the formula $[\text{MCp}^*_2][\text{MTCE}]$, $M = \text{Cr, Mn, and Fe}$. Functionally and electrochemically, MTCE is a hybrid between tetracyanoethylene (TCNE) and dimethyl dicyanofumarate (DMeDCF), two acceptors that have previously been found to support ferromagnetism. The X-ray crystal structure of the chromium analogue, $[\text{CrCp}^*_2][\text{MTCE}]$, shows it to exist in the expected mixed stack structure in the orthorhombic space group $Pnma$ with $a = 14.739(3) \text{ \AA}$, $b = 10.7869(19) \text{ \AA}$, and $c = 15.771(3) \text{ \AA}$ and $Z = 4$. As anticipated, all three family members exhibit dominant ferromagnetic coupling, which is presumed to reflect intrastack interactions. However, the bulk magnetic properties mostly differ from simple interpolations or extrapolations of the properties of their TCNE and DMeDCF analogues. Density functional theory calculations have been used to shed some light on this observation.

Introduction

Although through-bond magnetic coupling between two spin centers is a reasonably well-understood phenomenon, a generally accepted model of through-space coupling remains elusive because only noncovalent interactions are present, so the effort is a problem in both controlling weak exchange interactions and crystal engineering. Our approach to addressing this problem has been to prepare libraries of structurally or electronically related building blocks from which families of systematically modified charge-transfer (CT) salts can be constructed. Because the gross structural features in this class of compounds (mixed stacks with four stacks in each unit cell) are maintained across a wide variety of one-electron acceptor constituents, differences in magnetic properties should be ascribable to identifiable changes in crystal packing and electronic structure. Our idea is to use density functional theory calculations to determine spin density distributions and to correlate overlaps of regions of spin density between the donors and acceptors within a stack in comparable crystal structures with observed magnetic coupling.

Figure 1 illustrates a series of electron-poor olefins that have previously been employed in cycloadditions and copolymerization reactions.¹ Such compounds are also excellent one-electron acceptor building blocks for charge-transfer salt magnets. In particular, reactions between decamethylmetallocenes and tetracyanoethylene² (TCNE, **1**) or dimethyl dicyano-

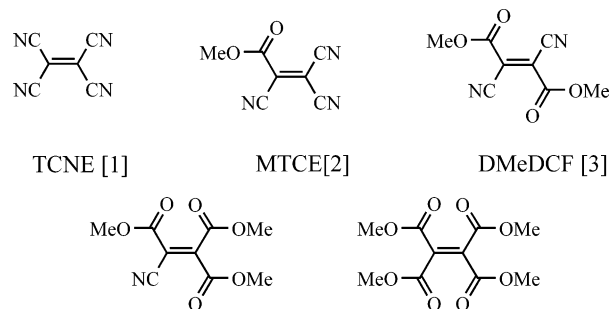


Figure 1. Examples of electron-poor acceptors.

fumarate (DMeDCF, **3**) yield families of ferromagnetically ordered solids, the latter reported by us.^{3,4} Specifically, $[\text{MnCp}^*_2][\text{TCNE}]$ ⁵ and $[\text{MnCp}^*_2][\text{DMeDCF}]$ ⁴ are glassy hard ferromagnets below 8.8 and 10.5 K, respectively, whereas $[\text{CrCp}^*_2][\text{TCNE}]$ ⁶ and $[\text{CrCp}^*_2][\text{DMeDCF}]$ ³ are soft ferromagnets below 3.65 and 5.3 K, respectively. For electrochemical reasons, FeCp^*_2 does not react with DMeDCF (vide infra), although it does react with TCNE to give a ferromagnet below 4.8 K.^{2,7}

- (2) Miller, J. S.; Calabrese, J. C.; Rommelmann, H.; Chittipeddi, S. R.; Zhang, J. H.; Reiff, W. M.; Epstein, A. J. *J. Am. Chem. Soc.* **1987**, *109*, 769–781.
- (3) Kaul, B. B.; Sommer, R. D.; Noll, B. C.; Yee, G. T. *Inorg. Chem.* **2000**, *39*, 865–868.
- (4) Kaul, B. B.; Durfee, W. S.; Yee, G. T. *J. Am. Chem. Soc.* **1999**, *121*, 6862–6866.
- (5) Yee, G. T.; Manriquez, J. M.; Dixon, D. A.; McLean, R. S.; Groski, D. M.; Flippen, R. B.; Narayan, K. S.; Epstein, A. J.; Miller, J. S. *Adv. Mater.* **1991**, *3*, 309–311.
- (6) Eichhorn, D. M.; Skee, D. C.; Broderick, W. E.; Hoffman, B. M. *Inorg. Chem.* **1993**, *32*, 491–492.
- (7) Taliaferro, M. L.; Selby, T. D.; Miller, J. S. *Chem. Mater.* **2003**, *15*, 3602–360.

[†] Virginia Polytechnic Institute and State University.

[‡] Howard University.

(1) Gotoh, T.; Padias, A. B.; Hall, H. K., Jr. *J. Am. Chem. Soc.* **1986**, *108*, 4920–4931.

The ester functional group in the fumarate acceptors is attractive because changing the alkyl group allows us to modify the structure without affecting the π network over which the unpaired spin is distributed. Thus, we have also investigated diethyl, di-*n*-propyl, and di-*i*-propyl analogues, and a paper on these studies is forthcoming.

Because the structural and electrochemical properties of methyl tricyanoethylenecarboxylate (MTCE, **2**)^{1,8,9} are intermediate between those of TCNE and DMeDCF, it represents a natural choice for examination as an acceptor. Hall and co-workers have reported the synthesis of MTCE by the acid-catalyzed metathesis between TCNE and methyl cyanoacetate.¹ Herein, we report the synthesis, characterization, and magnetic properties of the family of CT salts formed from this acceptor and commercially available decamethylmetallocenes, MCp^*_2 , $M = \text{Cr, Mn, and Fe}$.

Experimental Section

General Considerations. Preparations of air-sensitive compounds were carried out in a nitrogen-filled Vacuum Atmospheres glovebox and by utilizing standard Schlenk techniques. CrCp^*_2 , MnCp^*_2 , and FeCp^*_2 were purchased from Strem Chemicals. All other reagents were purchased from Aldrich or Alfa. Reagents were used as received except as noted below. Dichloromethane was distilled from P_2O_5 . Diethyl ether was distilled from Na/benzophenone. All solvents were degassed with glovebox N_2 prior to use. MTCE was synthesized by a previously published route,¹ except that purification was carried out by repeated recrystallizations from 5:1 hexanes/ether rather than by HPLC. It was judged to be pure by ^{13}C NMR. Elemental analyses were performed by Desert Analytics, Tucson, AZ.

Magnetic Measurements. All magnetic measurements were performed on a 5 T Quantum Design MPMS SQUID magnetometer (at NIST Gaithersburg) or a 7 T Quantum Design MPMS SQUID magnetometer. Measurements of magnetization as a function of temperature were performed from 1.8 to 300 K in 1000 or 5000 G applied field as indicated. Powder samples were cooled in zero applied field and measured upon warming. Samples were prepared as previously described.¹⁰ The amplitude of the oscillating magnetic field used for ac susceptibility measurements was 3.5 Oe with zero dc bias field and at frequencies of 1, 10, 100, and 1000 Hz. Diamagnetic corrections were applied on the basis of Pascal's constants for χT versus T plots, but no corrections were applied in the plots of M versus H or $ac\chi$ versus T data. In some cases, a linear offset was applied to the plot of the $ac\chi$ data for the sake of clarity.

X-ray Crystallography. Powder Diffraction. Compounds were sealed in 1.0 mm diameter glass capillaries (Blake Industries, Scotch Plains, NJ), and data were collected in transmission mode on an R-Axis Rapid diffractometer using copper radiation, a graphite monochromator, and a 0.5 mm incident beam collimator. The measurement conditions used $360^\circ \phi$ scans at $1^\circ/\text{min}$ with scan times ranging from 10 to 40 min depending on the diffracting nature of the samples. The data obtained were processed with the AreaMax¹¹ powder processing suite of programs.

Single-Crystal Diffraction. Dark red needles ($0.35 \times 0.024 \times 0.020$ mm³) were crystallized from CH_2Cl_2 /ether by vapor diffusion at room temperature in the glovebox. The chosen crystal was mounted on a nylon CryoLoop (Hampton Research) with Krytox Oil (DuPont) and centered on the goniometer of a Oxford Diffraction Xcalibur2 diffrac-

tometer equipped with a Sapphire 2 CCD detector. The data collection routine, unit cell refinement, and data processing were carried out with the program CrysAlis.¹² The Laue symmetry and systematic absences were consistent with the orthorhombic space groups $Pnma$ and $Pna2_1$. The centrosymmetric space group $Pnma$ was chosen on the basis of the $|E^2 - 1|$ value. The structure was solved by direct methods and refined using the SHELXTL NT program package.¹³ The asymmetric unit of the structure comprises 0.5 crystallographically independent $[\text{CrCp}^*_2][\text{MTCE}]$. The MTCE molecule disorders substantially, adopting two orientations with approximately the same footprint. The relative occupancies of the two orientations refined to 58.5% and 41.5%. Attempts to refine the structure with ordered MTCE molecules in other space groups were unsuccessful. The final refinement model involved anisotropic displacement parameters for the CrCp^*_2 , isotropic displacement parameters for the disordered MTCE, and a riding model for all hydrogen atoms. The program package SHELXTL NT was used for molecular graphics generation.

Modeling of Spin Density Distributions. The optimized geometry of the doublet radical anions of TCNE, MTCE, and DMeDCF was determined at the spin-unrestricted B3LYP^{14–16} level of theory using analytic energy gradients with Pople's standard 6-31+G* split-valence basis set.¹⁷ For each optimized structure, a Mulliken-like spin-population analysis was used to determine the spin density at each atom. The Gaussian98 suite of quantum chemical programs was used for all calculations.¹⁸

Synthesis. Decamethylchromocenium Methyl Tricyanoethylene-carboxylate, $[\text{CrCp}^*_2][\text{MTCE}]$. Decamethylchromocene (42 mg, 1.3×10^{-4} mol) was dissolved in 2 mL of CH_2Cl_2 . To this solution was added a solution of MTCE (24 mg, 1.5×10^{-4} mol) in 2 mL of CH_2Cl_2 . Immediately, the color of the solution turned from yellow to yellow-brown. After the solution was stirred for 0.5 h at room temperature, 10 mL of ether was added slowly to precipitate an air-sensitive yellow solid. The solid was filtered, washed with ether, and dried in a vacuum. Yield: 39 mg (61%). IR: $\nu(\text{CN})$, 2182 and 2136 cm^{-1} (sharp); $\nu(\text{CO})$, 1656 cm^{-1} (sharp). Anal. Calcd for $\text{C}_{27}\text{H}_{33}\text{CrN}_3\text{O}_2$: C, 67.06; H, 6.88; N, 8.69. Found: C, 66.84; H, 6.57; N, 8.60.

Decamethylmanganocenium Methyl Tricyanoethylenecarboxylate, $[\text{MnCp}^*_2][\text{MTCE}]$. Decamethylmanganocene (35 mg, 1.1×10^{-4} mol) was dissolved in 4 mL of CH_2Cl_2 , and the solution was cooled to -50°C . To this solution was added a solution of MTCE (17 mg, 1.1×10^{-4} mol) in 3 mL of CH_2Cl_2 , dropwise, while maintaining the temperature of the solution at -50°C . The solution turned brown. After the mixture was stirred for 0.5 h, 10 mL of ether was added slowly to yield a microcrystalline brown solid. After the solution was stirred for an additional 5 min, the precipitate was transferred to a Schlenk frit and filtered under vacuum. The solid on the frit was washed with 5 mL of cold ether, dried under vacuum for 1 h keeping the frit temperature at ca. -45°C , and finally dried at room temperature for 2 h. Yield: 38 mg (73%). IR: $\nu(\text{CN})$, 2183 and 2136 cm^{-1} (sharp);

(8) Hall, H. K., Jr.; Padias, A. B.; Way, T. F.; Bergami, B. *J. Org. Chem.* **1987**, *52*, 5528–5531.

(9) Yokozawa, T.; Tsuruta, E. *Macromolecules* **1996**, *29*, 8053–8056.

(10) Sellers, S. P.; Korte, B. J.; Fitzgerald, J. P.; Reiff, W. M.; Yee, G. T. *J. Am. Chem. Soc.* **1998**, *120*, 4662–4670.

(11) AreaMax, a suite of programs for analyzing and displaying powder diffraction data; MSC/Rigaku, 2002.

(12) CrysAlis v1.171; Oxford Diffraction: Wroclaw, Poland, 2004.

(13) Sheldrick, G. M. *SHELXTL NT ver. 6.12*; Bruker Analytical X-ray Systems, Inc.: Madison, WI, 2001.

(14) Parr, R. G.; Yang, W. *Density-Functional Theory of Atoms and Molecules*; Oxford University: New York, 1989.

(15) Lee, C.; Yang, W.; Parr, R. G. *Phys. Rev. B* **1988**, *37*, 785–789.

(16) Becke, A. D. *J. Chem. Phys.* **1993**, *98*, 5648–5652.

(17) Hariharan, P. C.; Pople, J. A. *Theor. Chim. Acta* **1973**, *28*, 213–222.

(18) Frisch, M. J.; Trucks, G. W.; Schlegel, H. B.; Scuseria, G. E.; Robb, M. A.; Cheeseman, J. R.; Zakrzewski, V. G.; Montgomery, J. A.; Stratmann, R. E.; Burant, J. C.; Dapprich, S.; Millam, J. M.; Daniels, A. D.; Kudin, K. N.; Strain, M. C.; Farkas, O.; Tomasi, J.; Barone, V.; Cossi, M.; Cammi, R.; Mennucci, B.; Pomelli, C.; Adamo, C.; Clifford, S.; Ochterski, J.; Petersson, G. A.; Ayala, P. Y.; Cui, Q.; Morokuma, K.; Malick, D. K.; Rabuck, A. D.; Raghavachari, K.; Foresman, J. B.; Cioslowski, J.; Ortiz, J. V.; Stefanov, B. B.; Liu, G.; Liashenko, A.; Piskorz, P.; Komaromi, I.; Gomperts, R.; Martin, R. L.; Fox, D. J.; Keith, T.; Al-Laham, M. A.; Peng, C. Y.; Nanayakkara, A.; Gonzalez, C.; Challacombe, M.; Gill, P. M. W.; Johnson, B. G.; Chen, W.; Wong, M. W.; Andres, J. L.; Head-Gordon, M.; Replogle, E. S.; Pople, J. A. *Gaussian 98*; Gaussian, Inc.: Pittsburgh, PA, 1998.

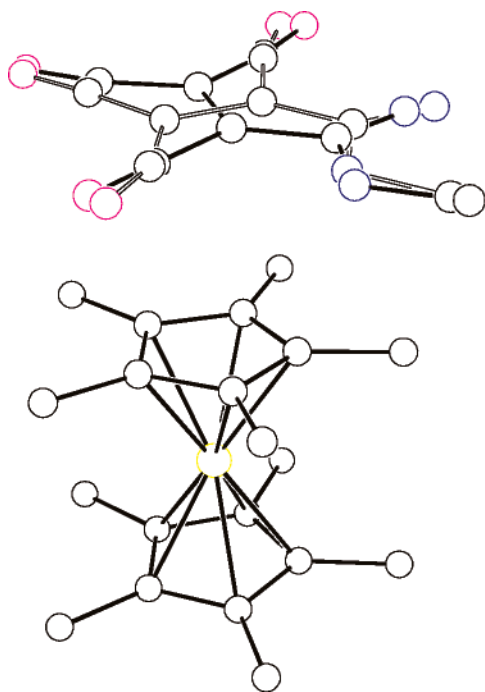


Figure 2. Asymmetric unit of $[\text{CrCp}^*_2][\text{MTCE}]$ illustrating the disorder in the anion radical.

$\nu(\text{CO})$, 1660 cm^{-1} (sharp). Anal. Calcd for $\text{C}_{27}\text{H}_{33}\text{MnN}_3\text{O}_2$: C, 66.66; H, 6.84; N, 8.64. Found: C, 66.28; H, 6.46; N, 8.06.

Decamethylferrocenium Methyl Tricyanoethylenecarboxylate, $[\text{FeCp}^*_2][\text{MTCE}]$. Decamethylferrocene (48 mg, 1.5×10^{-4} mol) was dissolved in 3 mL of CH_2Cl_2 . To this solution was added a solution of MTCE (24 mg, 1.5×10^{-4} mol) in 3 mL of CH_2Cl_2 . The color of the solution turned from yellow to yellow-green. After the solution was stirred for 0.5 h at room temperature, 5 mL of ether was added slowly to precipitate an air-sensitive, brown solid. The solid was filtered, washed with ether, and dried in a vacuum. Yield: 46 mg (64%). IR: $\nu(\text{CN})$, 2175 and 2138 cm^{-1} (sharp); $\nu(\text{CO})$, 1658 cm^{-1} (sharp). Anal. Calcd for $\text{C}_{27}\text{H}_{33}\text{FeN}_3\text{O}_2$: C, 66.53; H, 6.82; N, 8.62. Found: C, 66.17; H, 6.50; N, 8.96.

Results and Discussion

MTCE is an attractive acceptor for the synthesis of CT salt magnets for a number of reasons. Electrochemically, the first reduction potential of MTCE lies essentially in the middle between TCNE and DMeDCF.¹ As such, unlike DMeDCF, the reduction potential of MTCE is sufficiently positive to react with decamethylferrocene as well as the more strongly reducing Mn and Cr congeners, yielding three members of this family rather than two (Cr and Mn) as for DMeDCF. Furthermore, MTCE possesses the lowest symmetry of any acceptor to date, C_s , and the effects of this property are unknown.

The structure of $[\text{CrCp}^*_2][\text{MTCE}]$ has been determined by single-crystal X-ray diffraction. The compound exhibits the usual and expected stack of donors and acceptors related by two in-phase and two out-of-phase interstack interactions.³ The MTCE molecule is disordered over two nearly isosteric orientations that result from placement of the $\text{C}=\text{C}$ bond in two mutually orthogonal positions, which still allow near superposition of the three nitriles and ester group (Figure 2). The type of disorder, which is also seen with TCNE but not DMeDCF salts,³ occurs with nearly random occupancy of the two conformations and is expected to have an impact on the magnetic properties such

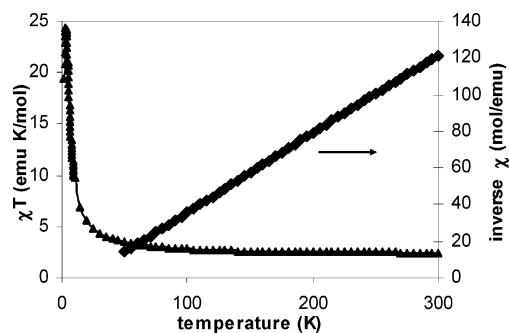


Figure 3. χT versus T (▲) and inverse χ versus T (◆) for $[\text{CrCp}^*_2][\text{MTCE}]$ measured in 1000 G.

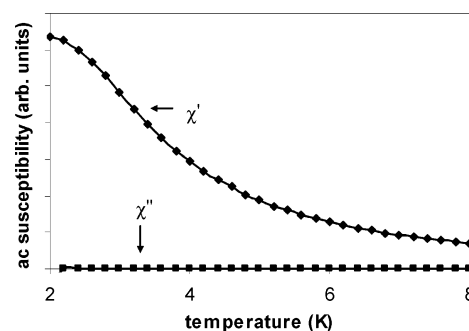


Figure 4. The ac susceptibility for $[\text{CrCp}^*_2][\text{MTCE}]$ at 1 Hz.

as frequency-dependent ac susceptibility. Powder diffraction measurements on all three congeners support the assertion that they are isomorphous¹⁹ and that the single-crystal solution is representative of the polycrystalline sample used for magnetic measurements. They also show that the manganese analogue is substantially less crystalline, presumably due to its low-temperature preparation method which for kinetic reasons would be expected to lead to smaller crystals.

Magnetic Properties. The chromium analogue in this family, $[\text{CrCp}^*_2][\text{MTCE}]$, possesses three unpaired electrons on the donor and one on the acceptor. An examination of the plot of χT versus T (Figure 3) shows ferromagnetic coupling with $\theta = 17\text{ K}$. Assuming the g -value for the organic radical is 2.0, the g -value for the chromocenium cation is calculated to be 2.04, consistent with the literature and the ^4A ground state of the metal complex.⁶ Although ferromagnetic coupling is present and a maximum is observed in χT versus T , the frequency-independent ac susceptibility data (Figure 4, 1 Hz data) exhibit only a point of inflection in χ' and no peak, indicating that this compound might be incipiently ordering at 1.8 K, the lowest temperature achievable. χ'' is zero at all temperatures. In contrast, based on interpolation of the properties of its TCNE and DMeDCF analogues, this compound was anticipated to be ordering at about 4 K.

The magnetic properties of the corresponding manganese analogue, $[\text{MnCp}^*_2][\text{MTCE}]$, are those of a glassy magnet, which is consistent with the behavior of the TCNE and DMeDCF analogues, although it exhibits an ordering temperature that is slightly lower than anticipated. The observed magnetic properties are reflective of the greater anisotropy seen for Mn(III) in this ligand field (with its ^3E ground state), as compared to Cr(III), which impacts the hysteresis that is observed in M versus H plots. As can be seen in the plots of χT

(19) See the Supporting Information.

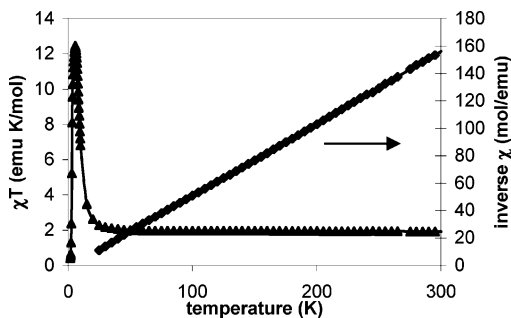


Figure 5. χT versus T (\blacktriangle) and inverse χ versus T (\blacklozenge) for $[\text{MnCp}^*_2][\text{MTCE}]$ measured in 1000 G.

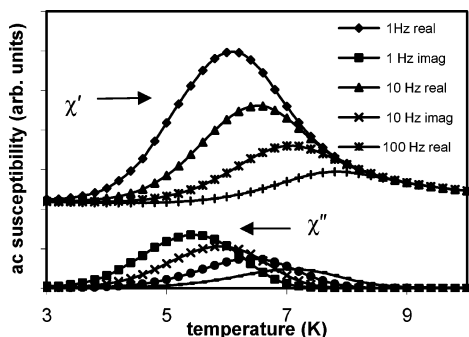


Figure 6. The ac susceptibility for $[\text{MnCp}^*_2][\text{MTCE}]$ at four different frequencies. Peaks flatten and shift to higher temperature with increasing frequency for both χ' (upper) and χ'' (lower).

versus T and χ^{-1} versus T measured at 1000 G (Figure 5), this compound also obeys the Curie–Weiss Law with $\theta = 3$ K, and, with the same assumptions as above, we calculate that $g = 2.48$ for the manganocenium cation.²⁰ There is a sharp increase below about 20 K, reaching a maximum at about 6 K. In contrast to the chromium analogue, strongly frequency-dependent ac susceptibility and nonzero χ'' (Figure 6) provide ample evidence of a transition to an apparent spin-glass state at about 7 K. The peaks in χ' and χ'' shift toward lower temperature with increasing frequency of the applied oscillating field, reflecting the fact that reorientation of the spins depends on how quickly they are being driven to change. $\Delta T_f/T_f \Delta \log \omega \approx 0.1$,¹⁹ a measure of the shift in the peak in χ' to higher temperature with increasing frequency, is consistent with a spin-glass-like state, resulting in part from the known disorder in the orientation of the MTCE anion.²¹ However, the plot of ΔT_f versus $\Delta \log \omega$ is distinctly nonlinear, indicating that this description is not completely adequate.¹⁹ The peak shifts with frequency are completely reproducible from preparation to preparation. The plot of M versus H measured at 1.8 K (Figure 7) shows significant hysteresis with $H_{\text{coer}} = 5.8$ kG. In contrast to its TCNE and DMeDCF analogues, which quickly reach saturation essentially at their respective coercive fields, the magnetization for $[\text{MnCp}^*_2][\text{MTCE}]$ is clearly far from saturation even at 70 000 G, our highest achievable field. This result also supports the greater glassy nature of the ordered state due to structural disorder. If, as it seems, the saturation magnetization

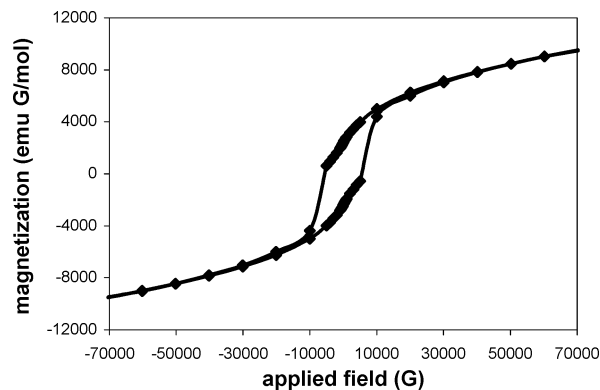


Figure 7. Magnetization versus applied field for $[\text{MnCp}^*_2][\text{MTCE}]$ measured at 1.8 K.

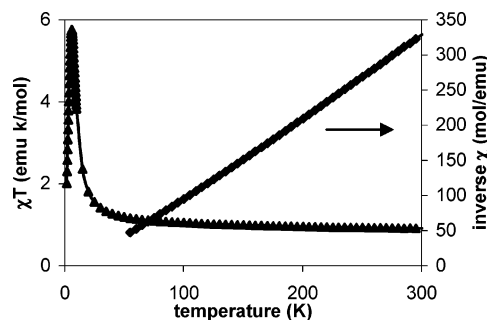


Figure 8. χT versus T (\blacktriangle) and inverse χ versus T (\blacklozenge) for $[\text{FeCp}^*_2][\text{MTCE}]$ measured in 5000 G.

would not reach ~ 19 000 emu G/mol (calculated from $g = 2.48$), then some canting of the moments must be present as is also seen with TCNE and DMeDCF.

The existence of canting is more clearly seen in the results of measurements on the iron analogue. The magnetic properties of $[\text{FeCp}^*_2][\text{MTCE}]$ are consistent with those of a noncollinear metamagnet, similar to those we reported for $[\text{FeCp}^*_2][\text{DCNQ}]$ ²² and not the expected ferromagnet.⁷ In a metamagnet, the ground state is antiferromagnetic in the absence of an applied field, and application of a magnetic field above a critical field, H_c , produces a ferromagnet-like state. In the present case, apparent canting of the moments in the nominally antiferromagnetic state produces a weak ferromagnet as indicated by remanence in zero applied field.

The plots of χT versus T and χ^{-1} versus T measured at 5000 G are shown in Figure 8. The χ^{-1} data can be fit to a Curie–Weiss expression with $\theta = 18$ K and $C = 0.87$ emu K/mol. Assuming the g -value for the organic radical is 2.0, the g -value for the ferrocenium cation is 2.3. The χT product grows to a maximum of 5.8 emu K/mol at about 6 K, whereupon an apparent antiferromagnetic phase transition takes place. This is most evident in the ac susceptibility, which shows a frequency-independent broad peak in χ' at about 5.7 K (Figure 9). This maximum is accompanied by the onset of nonzero χ'' at about this same temperature. Nonzero χ'' , indicative of hysteresis, is ordinarily not associated with an antiferromagnetic phase transition. To rationalize this observation, we assume that in the nominally antiferromagnetically ordered state, canting gives rise to incomplete cancellation of the magnetic moments. The remanance at 2.0 K is only 100 emu G/mol, and the coercive

(20) The χT data are complicated by a temperature-independent paramagnetism term that we can neither eliminate nor explain, but this has been seen previously. See: Da Gama, V.; Belo, D.; Santos, I. C.; Henriques, R. T. *Mol. Cryst. Liq. Cryst. Sci. Technol., Sect. A* **1997**, *306*, 17. For this analysis, we have subtracted out this component to yield a linear inverse χ versus T plot and a g value that is consistent with the literature.

(21) Mydosh, J. A. *Spin Glasses: an Experimental Introduction*; Taylor & Francis: London, 1993; pp 66–67.

(22) Yee, G. T.; Whitton, M. J.; Sommer, R. D.; Frommen, C. M.; Reiff, W. M. *Inorg. Chem.* **2000**, *39*, 1874–1877.

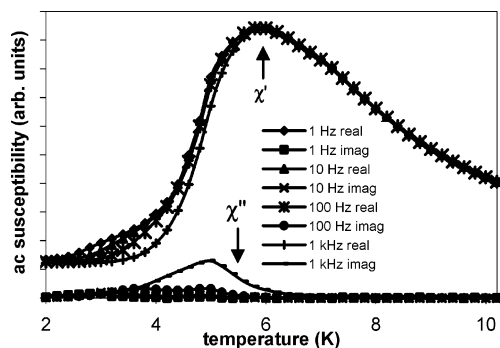


Figure 9. The ac susceptibility for $[\text{FeCp}^*_2][\text{MTCE}]$ at four different frequencies. The peak in χ'' decreases with increasing frequency.

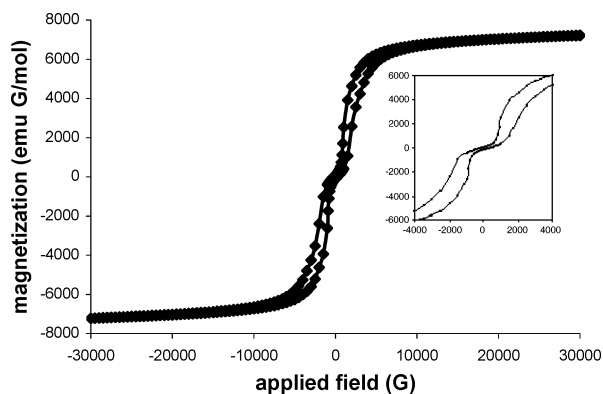


Figure 10. Magnetization versus temperature for $[\text{FeCp}^*_2][\text{MTCE}]$ measured at 2 K. Inset: expansion of data between ± 4000 G.

field is 250 G due to this feature (Figure 10). The plot of M versus H at 2.0 K shows that the critical field for the antiferromagnet-to-ferromagnet-like phase transition (given by the inflection point in this plot) is about 2 kG. The magnitude of the saturation magnetization (~ 7200 emu G/mol) is well below that expected ($\sim 12\,000$ emu G/mol) for collinear moments, again supporting canting.

In summary, to our surprise, the magnetic properties in this family of compounds were not those expected on the basis of a simple interpolation/extrapolation of the properties of the corresponding TCNE and DMeDCF salts. Arguably, the best “behaved” is the Mn analogue, whose properties are quite reminiscent of its TCNE and DMeDCF analogues except for the fact that the transition temperature is slightly lower than expected. Although the greater glassiness (shift in χ' with frequency) for the Mn analogue (as compared to DMeDCF) can be explained by the increased structural disorder, it is known that the TCNE analogue is also disordered with frequency-dependent ac susceptibility, the peak in χ' displaying a shift to higher temperature with increasing frequency (Figure 11). Also, it is possible that the solvent of crystallization, which has been shown to affect T_c , might play a role for the TCNE analogue,⁷ whereas there are no solvent molecules in the crystal structures of the MTCE and DMeDCF analogues.

Although MTCE lies electrochemically between TCNE and DMeDCF, we have found that, magnetically, the radical anion does not represent a simple mean between two extremes. Density functional theory calculations can be used to compare the distribution of unpaired spin density on TCNE, MTCE, and DMeDCF radical anions. These, in turn, are important in determining the magnitude of the exchange coupling via the

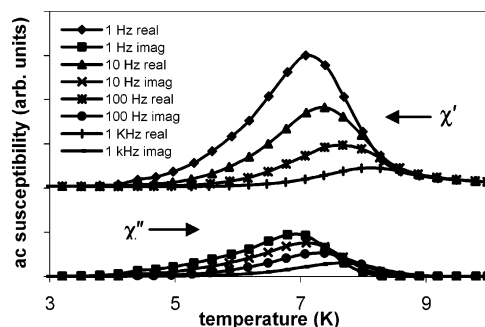


Figure 11. The ac susceptibility for $[\text{MnCp}^*_2][\text{TCNE}]$ at four different frequencies. Peaks flatten and shift to higher temperature with increasing frequency for both χ' (upper) and χ'' (lower).

Table 1. Atomic Spin Density Distribution for Three Related Acceptor Radical Anions (as a Fraction of One Spin)^a

	TCNE	MTCE	DMeDCF
ethylene carbon	0.377	0.426(d), 0.291(m)	0.325
nitrile nitrogen	0.164	0.185(c), 0.173(t), 0.127(g)	0.156
carbonyl oxygen		0.074	0.083
nitrile carbon	-0.103	-0.153(c), -0.105(t), -0.075(g)	-0.085

^a d, dicyano substituted; m, monocyano substituted; c, cis to ester; t, trans to ester; g, geminal to ester.

overlap of positive and negative spin density within the context of the McConnell I mechanism.^{23,24} Previous DFT calculations on $\text{TCNE}^{\cdot-}$ compare favorably with neutron diffraction data.²⁴ What the present results show is that for all three radical anions, the spin resides predominantly on the olefinic carbon atoms, with lesser amounts on the nitrile nitrogen atoms and carbonyl oxygen atom. From the data in Table 1, however, one can see that the distribution is substantially asymmetric and more extreme for MTCE; although the (geometric or arithmetic) mean of the significant positive spin densities for MTCE is intermediate between that for TCNE and DMeDCF, the actual values lie outside the range of either. This is also true for the negative spin density, which essentially only occurs on the nitrile carbon atoms in all three molecules, except that the mean is not intermediate, but is instead greater than that for TCNE. Thus, although we cannot yet explain our results, it is perhaps not so surprising that the magnetic properties are not as expected.

Conclusions

We investigated the family of compounds based on decamethylmetallocenes and methyl tricyanoethylenecarboxylate with the hope of discovering systematic trends relative to their TCNE and DMeDCF analogues. Although the crystal packing of donors and acceptors occurs exactly as predicted and the family of three compounds appears isomorphous, the magnetic properties differ from expectation. $[\text{CrCp}^*_2][\text{MTCE}]$ is not ordered above 1.8 K but appears to be an incipient magnet; $[\text{MnCp}^*_2][\text{MTCE}]$ appears to be a glassy ferromagnet below about 7 K; and $[\text{FeCp}^*_2][\text{MTCE}]$ is a canted metamagnet with an antiferromagnetic transition at 5.7 K. Because these results are not entirely consistent with expectations based on interpolation/extrapolation of previous results, we hypothesize that the magnetic properties of these compounds are a reflection of the

(23) McConnell, H. M. *J. Chem. Phys.* **1963**, *39*, 1910.

(24) Schweizer, J.; Bencini, A.; Carbonera, C.; Epstein, A. J.; Golhen, S.; Lelievre-Berna, E.; Miller, J. S.; Ouahab, L.; Pontillon, Y.; Ressouche, E.; Zheludev, A. *Polyhedron* **2001**, *20*, 1771–1778.

details of the spin density distributions on the MTCE radical anion, which we calculate to be not simply intermediate between those of TCNE and DMeDCF.

Acknowledgment. We acknowledge financial support from the donors of the Petroleum Research Fund, administered by the American Chemical Society (PRF 34614-AC to G.T.Y.), the National Science Foundation (CHE-023488 for the purchase of the SQUID and CHE-0131128 for the purchase of the Oxford Diffraction Xcalibur2 single-crystal diffractometer), and the ASPIRES program at Virginia Tech. We also thank Dr. Robert Shull of the National Institute of Standards and Technology,

Gaithersburg, MD, for use of the SQUID magnetometer for gathering preliminary data and Professor K. Travis Holman, Georgetown University, for the use of the powder diffractometer.

Supporting Information Available: X-ray crystallographic details (in CIF format) for $[\text{CrCp}^*_2][\text{MTCE}]$, powder diffraction patterns of all three compounds, simulation of powder diffraction based on the data from the single-crystal analysis, and a plot of $\Delta T_i/T_i \Delta \log \omega$ for $[\text{MnCp}^*_2][\text{MTCE}]$. This material is available free of charge via the Internet at <http://pubs.acs.org>.

JA0457213